AFRL-VS-TR-2002-1007

AFRL-VS-TR-
2002-1007

A SYSTEMS ENGINEERING STUDY OF GOSSAMER OPTICAL SATELLITES

Lawrence M. Robertson III

January 2002

Final Report

AIR FORCE RESEARCH LABORATORY
Space Vehicles Directorate
3550 Aberdeen Ave SE
AIR FORCE MATERIEL COMMAND
KIRTLAND AIR FORCE BASE, NM 87117-5776

AFRL-VS-TR-2002-1007

Using Government drawings, specifications, or other data included in this document for any purpose other than Government procurement does not in any way obligate the U.S. Government. The fact that the Government formulated or supplied the drawings, specifications, or other data, does not license the holder or any other person or corporation; or convey any rights or permission to manufacture, use, or sell any patented invention that may relate to them.

This report has been reviewed by the Public Affairs Office and is releasable to the National Technical Information Service (NTIS). At NTIS, it will be available to the general public, including foreign nationals.

If you change your address, wish to be removed from this mailing list, or your organization no longer employs the addressee, please notify AFRL/VSSV, 3550 Aberdeen Ave SE, Kirtland AFB, NM 87117-5776.

Do not return copies of this report unless contractual obligations or notice on a specific document requires its return.

This report has been approved for publication.

LAWRENCE M. ROBERTSON III
Project Manager, Advanced Mirror Systems

KIRT S. MOSER, DR-IV
Chief, Spacecraft Technology Division

REPORT DOCUMENTATION PAGE

Form Approved
OMB No. 0704-0188

1. REPORT DATE *(DD-MM-YYYY)*	2. REPORT TYPE	3. DATES COVERED *(From - To)*
02-01-2002	Final Report	10-01-2001 to 02-01-2002

4. TITLE AND SUBTITLE
A Systems Engineering Study of Gossamer Optical Satellites

5a. CONTRACT NUMBER

5b. GRANT NUMBER

5c. PROGRAM ELEMENT NUMBER
62601F

6. AUTHOR(S)
Lawrence Robertson

5d. PROJECT NUMBER
8809

5e. TASK NUMBER
LM

5f. WORK UNIT NUMBER
ZZ

7. PERFORMING ORGANIZATION NAME(S) AND ADDRESS(ES)

AFRL/VSSV
3550 Aberdeen Ave. SE
Kirtland AFB, NM 87117-5776

8. PERFORMING ORGANIZATION REPORT NUMBER

9. SPONSORING / MONITORING AGENCY NAME(S) AND ADDRESS(ES)

10. SPONSOR/MONITOR'S ACRONYM(S)

11. SPONSOR/MONITOR'S REPORT NUMBER(S)
AFRL-VS-TR-2002-1007

12. DISTRIBUTION / AVAILABILITY STATEMENT
Approved for Public Release; Distribution is Unlimited.

13. SUPPLEMENTARY NOTES

14. ABSTRACT

This paper describes a systems engineering modeling effort for very large, Gossamer, space optical systems. The focus of this effort was to determine the effect proposed Gossamer technology has on top-level performance parameters and total systems weight and power. For each technology chosen, system performance was evaluated using "first principals" approaches and then de-convolved into its specific hardware items. These specific hardware items and their performance, once identified, were flowed up into a single payload weight estimate. The payload weight was then combined with mission and spacecraft performance variables to create a single satellite system weight estimate. Finally, sensitivity of payload performance parameters within the payload weight estimate was performed in an attempt to understand the importance of the assumed technology performance.

15. SUBJECT TERMS
Telescopes, Mirrors, Structures

16. SECURITY CLASSIFICATION OF:			17. LIMITATION OF ABSTRACT	18. NUMBER OF PAGES	19a. NAME OF RESPONSIBLE PERSON
a. REPORT	b. ABSTRACT	c. THIS PAGE			Lawrence Robertson
Unclassified	Unclassified	Unclassified	SAR	28	19b. TELEPHONE NUMBER *(include area code)* (505) 846-7687

Table of Contents

List of Tables

List of Figures

1. Introduction

This paper describes a systems engineering modeling effort for very large, Gossamer, space optical systems. Figure 1-1 shows an artists rendition of such a system. The focus of this effort was to determine the effect proposed Gossamer technology has on top-level performance parameters and total system weight and power. For each technology chosen, system performance was evaluated using "first principals" approaches and then de-convolved into its specific hardware items. These specific hardware items and their performance, once identified, were flowed up into a single payload weight estimate. The payload weight was then combined with mission and spacecraft performance variables to created a single satellite system weight estimate. Finally, sensitivity of payload performance parameters within the payload weight estimate was performed in an attempt to understand the importance of the assumed technology performance.

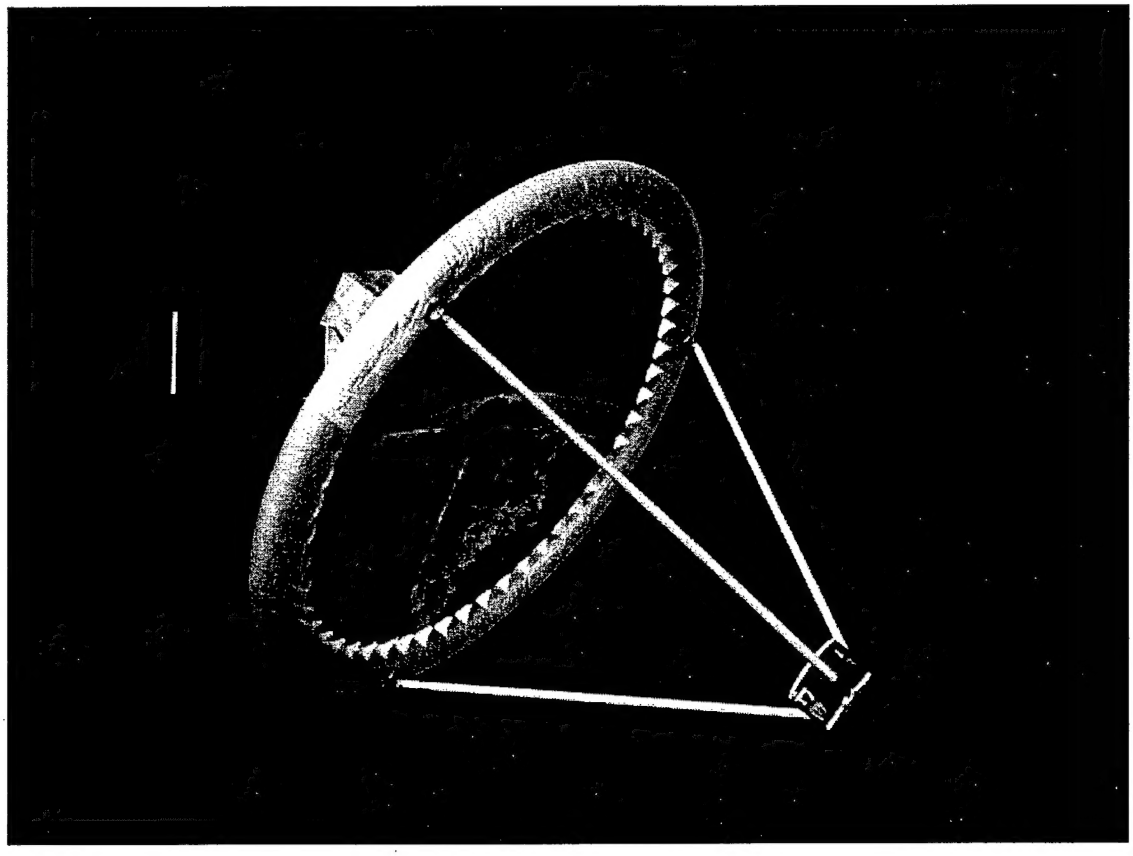

Figure 1-1. A Gossamer space imaging system

As a starting point, the Aerospace Corporation's Deployable Optics Concurrent Engineering Model (CEM) was used for this study [1], [2]. The original CEM incorporated key iterative spacecraft weight equations, large aperture performance results, and payload component lists to create performance and weight estimates for large aperture, deployable aperture systems. The model allowed the user to vary everything from specific COTS spacecraft hardware to payload performance parameters. The user-

defined choices translated into component weights that were then rolled up into an iterative calculator that determined the total system weight. New payload technology can be added to the CEM by simply adding new choices to the payload section.

Telescope Mass Properties

Parameters Tied to Other Sheets Used by This Sheet	
Aperture Size	26.00 m
Secondary Mirror Boom Weight (3)	7976.60
Number of Primary Mirror Booms	10.00
Primary Mirror Boom Weight	**266.70** kg
Primary Mirror Areal Density	**12.66**

	Parameters	Areal density [kg/m^2]	Total [kg]	Margin	Mass [kg]	Power [W]
Optical Components (Not Including Secondary)			**98.17**		**233.81**	**30.00**
Primary Mirror	Membrane - Electrostrictive (E-Gun)				106.19	13.30
Secondary Mirror (Covered Below)						
Tertiary	Dia [m] 1.00 Area [m^2] 0.79	50.00	39.27	0.25	49.1	
Aft Optical Elements	Dia [m] 0.50 Area [m^2] 0.20	100.00 2	39.27	0.25	49.1	
Fast Steering Mirror	Dia [m] 0.50 Area [m^2] 0.20	100	19.63	0.5	29.5	30.0
Primary Mirror Support Structure		Quanity	**423.27**		**6615.28**	**1250.00**
Deployment Mechanisms	L'Garde -Spiral oragami with inflatable I		**6615.28**		6615.28	1210.00
Secondary Mirror and Support Structure			**105.56**		**10614.59**	**0.00**
Secondary Mirror	Dia [m] 2.00 Area [m^2] 3.14	28.00	87.96	0.25	110.0	
Non-Contact Primary Mirror Control Mechanicsm					1186.2	
Secondary Bi-Pod Actuators	Mass [kg] 0.30	0	0.00	0.25	0.0	0.0
Secondary Reaction Support Interface			17.59	0.3	22.9	
Subtotal of Secondary Mirror Mass					1319.0	
Secondary Trusses (Analysis from Primary Mirror Support Structure Sheet)					7976.6	
Other Equipment			**106.08**		**146.90**	
Thermal Control Hardware			10.00	0.5	15.0	40.0
Spacecraft Interface / Optical Bench			61.08	0.3	79.4	
Sunshade/baffle			35.00	0.5	52.5	
Contamination Covers			0.00	0.25	0.0	
Phasing Equipment & Electronics		Quanity	**273.89**		**512.44**	**255.24**
Control Electronics, Digital Signal Proc	Mass [kg]: 2.00 Power [W] 40.00	2	4.00	0.25	5.0	80.0
Cabling	ensity [kg/m] 0.20 Length [m] 936.000		187.20	1	374.4	
Alignment Source and Beam Launcher	Mass [kg]: 2.70	6	16.20	0.5	24.3	20.0
Alignment Sensor Heads	Mass [kg]: 2.00	6	12.00	0.5	18.0	2.0
Phasing Initialization & Calibration H/W			0.00	0.5	0.0	
Deformable Mirror			20.00	1	40.0	40.0
LOS Reference Unit			0.00	1	0.0	0.0
Engineering Measurement System			10.00	0.25	12.5	40.0
Low Powered Laser			5.00	1	10.0	50.0

Figure 1-2. Telescope spreadsheet of the CEM

The Gossamer study involved modifying the CEM payload weight and performance estimates to include new technology. The telescope spreadsheet of the new CEM, where the payload weight is calculated, was broken out into two separate spreadsheets: a primary mirror spreadsheet and support structures spreadsheet. The primary mirror spreadsheet contained all of the current state-of-the-art mirror technology performance and weight equations with new mirror technology such low areal density membrane optics and figure control systems with electron gun electrostrictive control systems. Similarly, the boundary and support structures spreadsheet contained all of the deployable optics technology, but now included options for membrane boundary systems such as inflatable rigidizable torus support structures or boom type of structures. These new additions captured all of the hardware needed for a large Gossamer system. As before, the payload weight and power estimates were flowed up to the spacecraft systems sheet, where final iterations on system weight were performed.

Figure 1-2 shows a portion of the spacecraft spreadsheet of the CEM Excel spreadsheet. In general, red cells are user-defined inputs, pink cells are calculated values based on other spreadsheets or cells, and green cells are comment areas. Besides spacecraft component choices, the CEM spacecraft spreadsheet calculates propulsion weight and the final satellite weight. Other sheets that feed the spacecraft spreadsheet include the telescope sheet, a primary mirror and phasing actuators sheet, a primary mirror support and deployment structure sheet, an optics sheet, and several cost and data sheets. Specific details about the new support structure and primary mirror sheets are provided below.

2. Primary Mirror Support and Deployment Spreadsheet

To support the primary mirror system any large aperture system must contain a support structure to deploy and hold the primary mirrors in place. The Primary Mirror Support and Deployment spreadsheet within the Gossamer CEM captured the performance, weight and power assessment of this subsystem. This sheet outlined all of the hardware needed to deploy and support the primary mirror. Boundary control hardware was also included in this sheet.

Three individual technology choices were available from this sheet: a spiral origami inflatable rigidizable torus, deployable booms for a membrane system, and deployable booms for a rigid-mirror, segmented-ring deployable optic. In general, deployable boom calculations for the segmented-ring and membrane mirror are similar, with major differences being in the tip masses used and the number of booms used to support the primary mirror.

2.1 Spiral Origami Support Structure

Figure 2 shows an example of this type of support structure. The identified hardware items for this system were the torus, the inflation gas, the lifetime gas, the tank for the inflation gas, the tensioning hardware, the plumbing hardware and the secondary tower. The torus size is based on the cross-sectional radius being one-tenth the diameter of the telescope. Using this assumption, the torus volume is given by:

$$V = 2\pi^2 Rr^2 = 2\pi^2 R^3 / 100 \tag{2.1-1}$$

where R is the radius of the primary mirror and r is the radius of the cross-sectional area of the torus. The lifetime gas was estimated to be 12 times that of the original volume. The mass of the gas was estimated using the ideal gas law of

$$m = \frac{pV}{RT} \tag{2.1-1}$$

where R is the specific gas constant for Nitrogen of 55.2 ft-lbf/lbm-R, T is –120 degrees F and p is 0.0004 psi. The tank volume was estimated using the same formula above accept the storage temperature and pressure was estimated to be 70 degrees F and 73.5 psi. The tank weight can then be estimated using,

$$r = \left(\frac{3}{4\pi} V\right)^{1/3} \tag{2.1-1}$$

as the radius of the tank and

$$SA = 4\pi r^2 \tag{2.1-1}$$

for the surface area of the tank. The tank weight can then be calculated by knowing the wall thickness and the density of the material, which was assumed to be 1mm and 2850 kg/m^3 respectively. The torus weight was calculated using the equation for the surface area of a torus, which is

$$SA = 2\pi rR = 0.2\pi R^2 \tag{2.1-1}$$

and 0.2 kg/m^2 as the weight density of the torus material. The plumbing was assumed to weigh about 1.2 kg, while the tensioning hardware was assumed to weigh about 0.3 kilograms per actuator with 12 actuators needed. Each actuator was assumed to need 5 Watts of power, while the inflation system was assumed to need 10 Watts. The power needed by the inflation system could not be verified. Many of the assumptions about the torus hardware were taken from [3] while the actuation hardware is traceable to PNM hardware available from Xinetics. All the equations shown are simple Calculus derived equations commonly found in any introductory engineering textbooks.

2.2 Boom Supported Membrane

The booms-supported membrane equations are based on [4] and use four basic performance parameters to determine the boom weight. For each set of equations, the boom thickness was isolated as the only dependant parameter and then solved for using set performance metrics. The highest thickness number from the four performance equations was used as the final boom thickness. Independent parameters such as the number of booms, was set to a single number varied during the sensitivity study. Table 2.2 shows some of the assumed performance parameters and the reasons for the choices.

Table 2.2-1. Values used for the boom support structure

Parameter Name	Symbol	Nominal Value	Units	Reason for Value	Sensitivity Parameter
Obscuration Size	L_o	1	M	Arbitrary	N
Momentum Wheel Torque	T_w	0.04	N-m	Based on hardware	N
Momentum Wheel Speed	f_w	50	Hz	Arbitrary	N
Momentum Wheel Mass	f_m	3.825	Kg	Based on hardware	N
Axial Boom Frequency	f_a	5	Hz	A little low for launch but booms supported with fairing h/w	Y
Lateral Boom Frequency	f_l	5	Hz	A little low for launch but booms supported with fairing h/w	Y
Boom Radius to Thickness Ratio	R_t	10	(none)	Must be greater than 10 for assumptions	Y
Modulus	E	7.1E10	N/m^2	Al modulus. Also modulus consistent with weakest possible composite axis	N
Density	p	1.66E03	Kg/m^3	Composite material	N
Max Boom Deflection from Disturbance	d_w	1e-05	m	Range of fast actuator	N
Number of Booms	N_b	8	(none)	Based on reasonable reduction of wrinkling	Y
Ultimate Tensile Strength	F_{tu}	5.24E08	N/m^2	Based on reference	N

The first design parameter used to determine the weight of the booms was deflection of the boom from the momentum wheel imbalance disturbance. The deflection of a boom with a tip mass at the end is given by

$$d_w = \frac{L^3}{EI}\left(\left(\frac{T_m}{3} + \frac{(B_m + D_m)}{12}\right)(a_L + w(L + L_v + 0.5L_o))\right) \tag{2.2-1}$$

where L is the boom length, I is the cross sectional area inertia, E is the material modulus, T_m is the tip mass, B_m is the boom mass, D_m is non-boom distributed mass, L_v is the vertical distance from the momentum wheel to the boom attachment point, L_o is the obscuration size, w is the angular acceleration component of the momentum wheel noise given by

$$w = 0.00000028 f_w^2 m_w / I_s \tag{2.2-2}$$

and a_L is the acceleration component of the momentum wheel noise given by

$$a_L = 0.00000025 f_w^2 m_w / m_s \tag{2.2-3}$$

where f_w is the wheel speed, m_w is the wheel mass and I_s and m_s are the satellite mass and inertia. The wheel noise acceleration terms are estimated from data with the constants having appropriate units.

If the radius to thickness ratio of the boom R_t is set to 10 then the cross sectional area inertia can be written as

$$I = \frac{\pi}{4}\left(R^4 - (R-t)^4\right) = \frac{\pi}{4}\left(R^4 - R^4 + 4R^3 t + \ldots\right) \approx \pi R_t^3 t^4 \tag{2.2-4}$$

where t is the boom thickness. The boom mass can also be written as

$$B_m = 2\pi L R_t \rho t^2 \tag{2.2-5}$$

where p is the material density. Solving for the boom thickness

$$\frac{d_w E \pi R_t^3}{L^3(a_L + w(L + L_v + 0.5L_o))} t^4 - \frac{1}{6}\pi L R_t \rho t^2 - \left(\frac{T_m}{3} + \frac{D_m}{12}\right) = 0 \tag{2.2-6}$$

simplifies the problem into solving a quadratic equation. This equation specifies the boom thickness needed given a tip mass displacement.

The second design parameter used to determine the weight of the booms was deflection of the boom from a slew maneuver. Boom thickness was found similar to the above equations accept the deflection caused by a slew is given by:

$$d_s = \frac{L^3}{EI}\left(\left(\frac{T_m}{3} + \frac{(B_m + D_m)}{8}\right)\left(a_s\left(L + L_v + 0.5L_o\right)\right)\right) \tag{2.2-7}$$

The third parameter is the axial frequency of the boom, given by

$$f_a = 0.16\sqrt{\frac{AE}{L\left(T_m + 0.333(B_m + D_m)\right)}} \tag{2.2-8}$$

The boom mass is given by 2.2-5 but the cross sectional area is given by

$$A = \pi R_t^2 t^2 \tag{2.2-9}$$

Combining like powers of the thickness gives.

$$t = \sqrt{\frac{\left(\frac{f_A}{0.16}\right)^2 L\left(T_m + \frac{D_m}{3}\right)}{E\pi R_t^2 - \left(\frac{f_A}{0.16}\right)^2 \frac{2}{3}\pi\rho R_t L^2}} \tag{2.2-10}$$

This equation defines the axial boom frequency performance measure.

The fourth parameter is the lateral frequency of the boom, given by

$$f_L = 0.276\sqrt{\frac{EI}{L^3\left(T_m + 0.236(B_m + T_m)\right)}} \tag{2.2-11}$$

Combining like powers of the thickness gives.

$$\left(\frac{f_L}{0.276}\right)^2 \left(T_m + 0.236D_m\right)L^3 + \left(\frac{f_L}{0.276}\right)^2 (0.236)L^4 2\pi R_t \rho t^2 - E\pi R_t^3 t^4 = 0 \tag{2.2-12}$$

which can be used to solve for the thickness.

The fourth parameter used to size the boom thickness was stability of the boom. Stability refers to sizing the boom for the compressive buckling stresses that the boom may encounter. The critical buckling stresses on a boom are given by

$$\sigma_{cr} = 0.6\gamma \frac{Et}{R} \tag{2.2-13}$$

where γ is a factor used to correlate theory with results, t is the boom thickness, R is the boom radius and E is the boom material modulus. The factor γ is given by:

$$\gamma = 1 - 0.901\left(1 - \exp\left(-\frac{1}{16}\sqrt{R_t}\right)\right) \tag{2.2-14}$$

For equation 2.2-13, the other side of the critical compressive stress equation is given by:

$$P_{cr} = \sigma_{cr} A = 65(T_m + D_m + B_m) + \frac{60}{R_t t} L(T_m + 0.5(B_m + D_m)) \tag{2.2-15}$$

Solving for the boom thickness gives,

$$\pi R_t (130L\rho - \sigma_{cr})t^3 + (60L^2\pi\rho)t^2 + 65(T_m + D_m)t + \frac{60L}{R_t}(T_m + 0.5D_m) = 0 \tag{2.2-16}$$

or

$$t^3 + at^2 + bt + c = 0 \tag{2.2-17}$$

If the following substitution is made

$$y = t - \frac{a}{3} \tag{2.2-18}$$

then the solution for y is given by

$$y = \sqrt[3]{-\frac{q}{2} + \sqrt{\frac{q^2}{4} + \frac{p^3}{27}}} + \sqrt[3]{-\frac{q}{2} - \sqrt{\frac{q^2}{4} + \frac{p^3}{27}}} \tag{2.2-19}$$

via Cardan's formula [5], where

$$p = b - \frac{a^2}{3} \tag{2.2-20}$$

$$q = \frac{2a^3}{27} - \frac{ab}{3} + c \tag{2.2-21}$$

It was assumed that the other two roots contained complex numbers or where not the most conservative estimate.

The final parameter used to size the boom thickness was strength of the boom or the compressive stresses. The formulas are similar to those given for sizing the boom for stability accept the materials allowable stress is used instead of the buckling stress.

According to [4], the analysis for the strength and stability sizing is correct for only a limited number of conditions. The radius to thickness ratio must be less than 1500, which it is constrained to be, and the boom length to radius ratio must be less than 5, which most of the time it is not. Therefore, it was determined that another formula for examining the boom buckling must be used, with the largest thickness used to determine the appropriate boom sizing for stability.

From [6], a column in compression will fail at a critical or Euler buckling load, given by:

$$P_{cr} = \frac{\pi^2 EI}{L^2} = \frac{\pi^3 E R_t^3 t^4}{4L^2} \tag{2.2-22}$$

Using the right side of equation 2.2-15 as the critical load and equating like terms of the boom thickness becomes:

$$-\frac{\pi^3 E R_t^3}{4L^2} t^5 + 130 L \pi R_t \rho t^3 + \left(60 L^2 \pi \rho\right) t^2 + \tag{2.2-23}$$
$$65(T_m + D_m)t + \frac{60L}{R_t}(T_m + 0.5 D_m) = 0$$

The solution to a polynomial of power five cannot be found analytically. Therefore, an iterative method such as Picard's method must be used. Picard's method will only find real roots, which we are guaranteed to have at least one. Picard's method is given by:

$$x_{n+1} = x_n - \frac{f(x_n)}{\frac{df(x_n)}{dx}} \tag{2.2-24}$$

With an initial guess x0. The other four roots of the system can be found by recognizing that:

$$(t + r)\left(t^4 + et^3 + ft^2 + gt + h\right) = 0 \tag{2.2-25}$$

Where –r is the root found using 2.2-25 and

$$e = -r \tag{2.2-26}$$
$$f = a + r^2 \tag{2.2-27}$$
$$g = b - r\left(a + r^2\right) \tag{2.2-28}$$

$$h = c - r\left(b - r\left(a + r^2\right)\right) \tag{2.2-29}$$

The solution for a polynomial of power four can be found analytically [3] by first solving for

$$y^3 - fy^2 + (eg - 4h)y - \left(h\left(e^2 - 4f\right) + g^2\right) = 0 \tag{2.2-30}$$

using 2.2-17 thru 2.2-21. Next, using the equations

$$\alpha = \sqrt{\frac{e^2}{4} - f + y} \tag{2.2-31}$$

$$\beta = \sqrt{\frac{y^2}{4} - h} \tag{2.2-32}$$

The four solutions to 2.2-25 are

$$t^2 + \left(\frac{e}{2} \pm \alpha\right)t + \left(\frac{y}{2} \pm \beta\right) = 0 \tag{2.2-33}$$

In most cases the roots found in 2.2-33 are complex, but must be checked for real roots. Also the solution to 2.2-30 possibly contains other roots that also must be checked.

The analysis of the boom structure was also used to size the secondary mirror support arms. Assuming that an optical design can be constructed such that the position of the secondary mirror is equal to the half the diameter of the primary mirror, then the analysis for the primary mirror boom support arms can also be size the secondary mirror support struts. The number of secondary mirror support struts was assumed to be three.

3. Primary Mirror Aperture

The primary mirror aperture system was limited to a single configuration of a membrane mirror with shape control provided by an electron gun. Other technology such as electrostatic control was investigated but was discarded due to a lack of information on the specific hardware needed for such a system. Other options, such as advanced mirror technology, were also not included due to areal density concerns.

The hardware identified for an electrostrictive system where the membrane, the electron guns and the cabling for the guns. The wavefront sensing system was lumped into the phasing system for the telescope and therefore was not included in the weight of the primary mirror aperture. The membrane was assumed to weigh approximately 0.2 kg/m2 while the cabling for the electron gun was assumed to weigh 0.2 kg/m. Using a Kimbal Physics electron gun, the gun was found to weight 7.5 lbs. The key performance parameter for the system was discovered to be the coverage of the gun. Looking at

documentation such as [7], each gun was assumed to be able to handle 4 meters squared. This value drove the weight of this system. For example, a 26-meter diameter aperture requires 133 guns to control the entire surface. If the weight of the cables were included, the total weight was almost 1150 kgs. In comparison, the weight of the membrane was only 106 kg. The areal coverage of the electron guns was a key parameter identified for sensitivity analysis. The guns were assumed to reside on the secondary mirror system.

4. Sensitivity Analysis

Sensitivity analysis was performed in three different ways. First, sensitivity analysis was performed on parameters related to a boom structural support. Next, sensitivity analysis was performed on the torus support structure performance parameters. Finally, parameter variation studies were done on the primary mirror hardware itself. In all three cases, the dependant variable was the primary mirror areal density for a 26-meter aperture. Once the core parameters are identified, analysis of areal density as a function of aperture size also was performed.

4.1 Sensitivity Analysis of Boom Parameters

Using the formulas derived in section 2.2, sensitivity analysis was performed on several key parameters related to a boom support structure. Those parameters and value ranges are shown in Table 4.1-1. In all, over 300 scenarios were examined. The dependant variable was always areal density for an aperture size of 26 meters. Also, the lateral and axial frequency parameters were varied at the same time.

Table 4.1-1. Sensitivity parameters in boom study

Parameter Name	Symbol	Nominal Value	Units	Reason for Value	Range Values
Boom Radius to Thickness Ratio	R_t	10	(none)	Must be greater than 10 for assumptions	10 to 50 with step size of 10
Axial Boom Frequency	f_a	5	Hz	A little low for launch but booms supported with fairing h/w	0.5 to 5 with step size of 0.5
Lateral Boom Frequency	f_l	5	Hz	A little low for launch but booms supported with fairing h/w	0.5 to 5 with step size of 0.5
Number of Booms	N_b	8	(none)	Based on reasonable reduction of wrinkling	5 to 10 with step size of 1

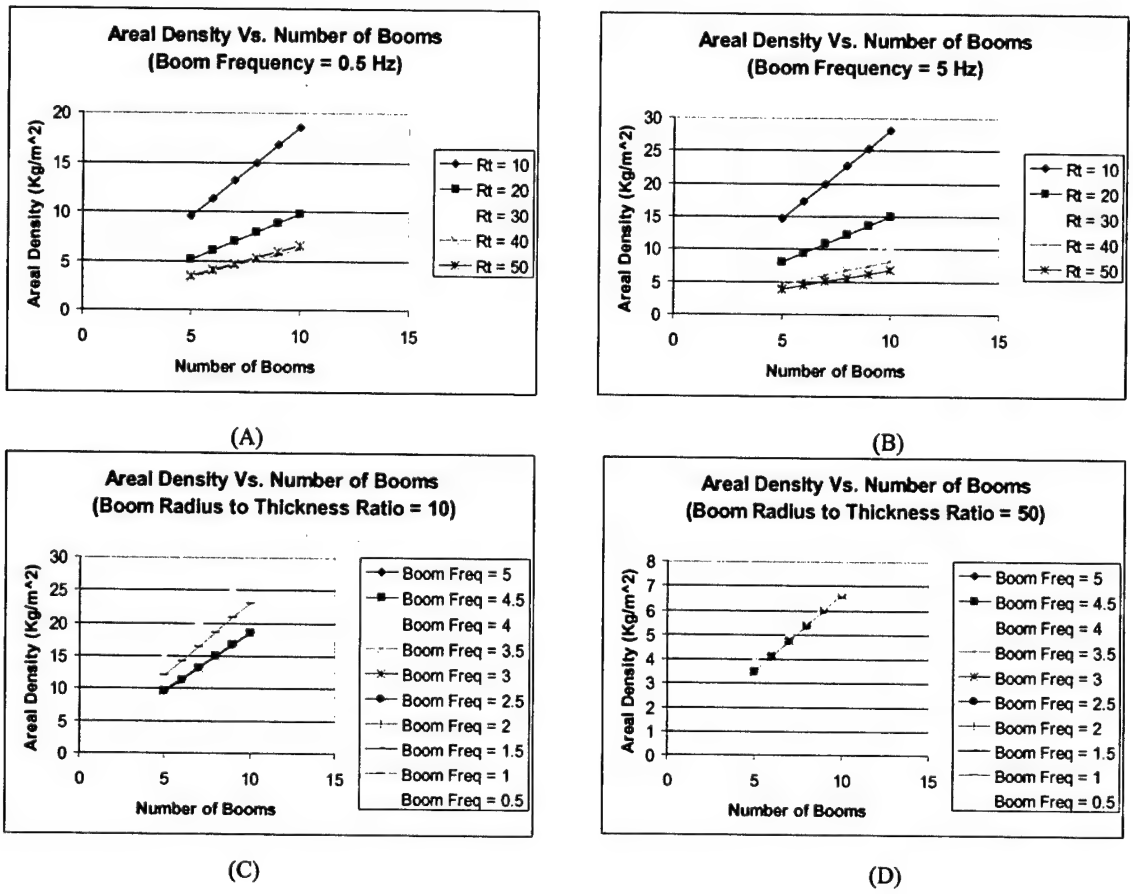

Figure 4.1-1. Aperture areal density versus number of booms

Figure 4.1-1 shows the dependence of the number of booms on the areal density given the boom frequency. Notice that as the number of booms increases, so does the areal density. For a boom radius-to-thickness ratio of 10, the areal density doubles when the number of booms doubles. This comparison is true for both extreme boom frequency choices shown. Also notice in Figure 4-1.4d how the frequency does not affect the areal density when the boom radius-to-thickness ratio is 50.

This effect of areal density versus boom first nature frequency is very apparent in Figure 4.1-2. Only at the high-end of values does boom frequencies have an effect on the aperture areal density. Most of this is caused by the boom stability being the major design parameter driving the boom thickness, making the boom frequency somewhat arbitrary.

Figure 4.1-3 shows the aperture areal density versus boom radius-to-thickness ratio plots. Notice how the Rt ratio is a key parameter for obtaining low aperture areal densities. The reasoning for this lies in the boom cross sectional inertia and boom weight calculations. In general, each boom factor has the boom cross sectional inertia as a key driver. The boom radius-to-thickness ratio is related to the cube of this ratio, while the boom mass is only directly proportional to the Rt ratio. Even though the inertia is not directly related to

each thickness calculation, the cross sectional inertia term plays a key role. The effect of the boom radius to thickness ratio also does have a local minimum for a low number of support booms and a low boom frequency. In Figure 4.1-3b and 4.1-3d the areal density reaches a local minimum of 3.5 kilograms per meter squared at an Rt of 40 and a boom frequency lower than 4 Hz.

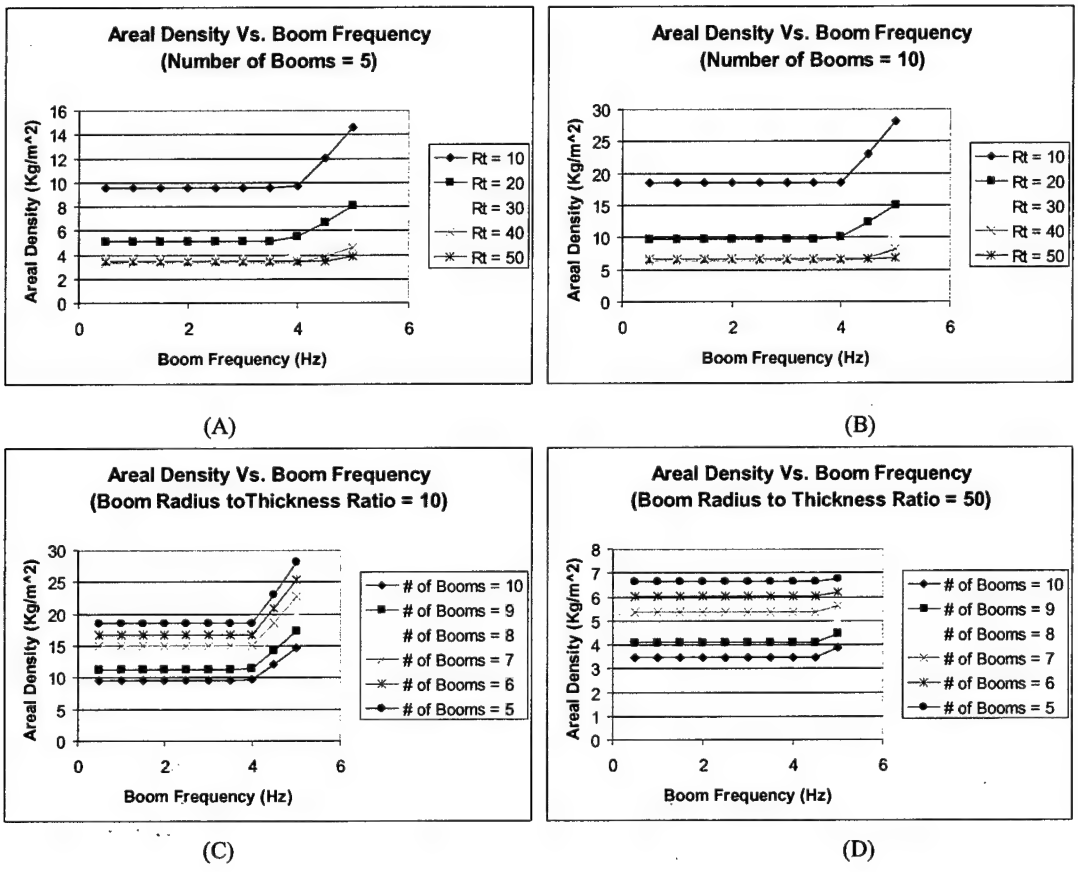

Figure 4.1-2. Aperture areal density versus boom frequency

4.2. Sensitivity of Spiral Origami Torus Support Structures

For the inflatable, rigidizable torus structure, there are a number of parameters that were proposed as variables in the sensitivity study. However, since this technology is very new, it was difficult to assess which parameters were real and which where unrealistic. Therefore, the margin associated with the weight of each parameter was varied at the same time and the aperture areal density plotted. The total weight specified for a piece of hardware is one plus the margin number times the original estimated weight of the item. A margin of 9 equates to a specified weight of 10-kilograms for a 1-kilogram piece of equipment. Figure 4.2-1 shows the results of this study.

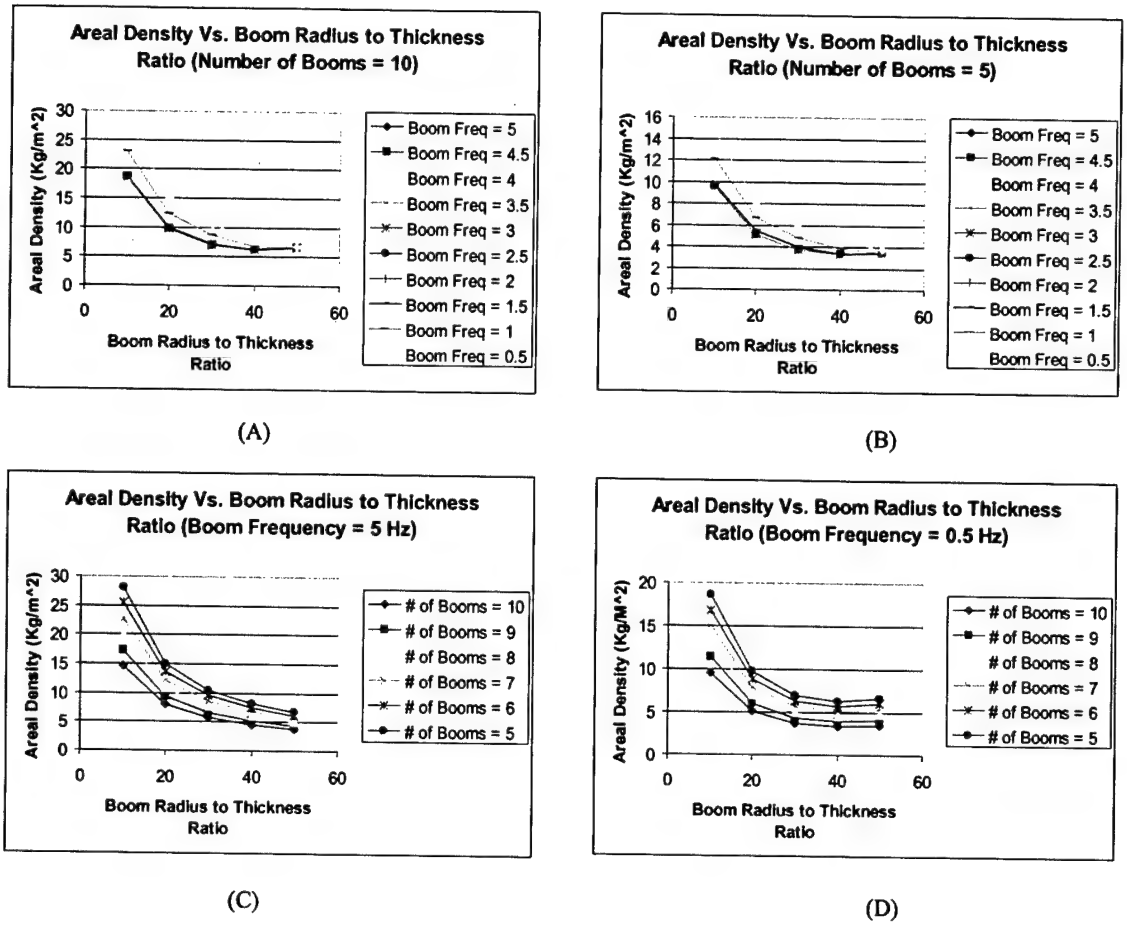

Figure 4.1-3. Aperture areal density versus boom radius to thickness ratio

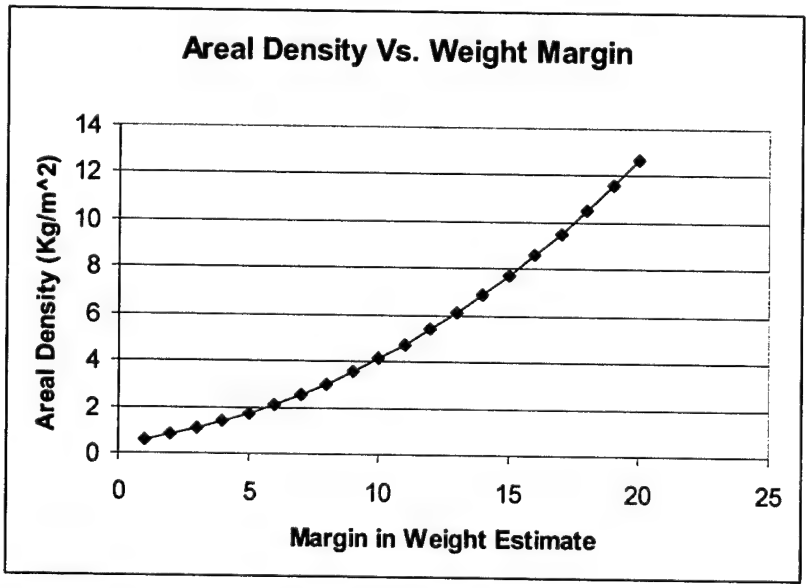

Figure 4.2-1. Areal density versus weight margin

Notice that for relatively high margins, that the areal density is still quite low. Weight values ten times higher than those estimated still give produce areal densities lower than 4. This suggests that this technology is superior to boom supports if one, the membrane and torus can be packaged such that wrinkling is minimized and two; the torus frequencies are high enough to withstand slewing and/or momentum wheel disturbances.

4.3. Sensitivity of the Primary Mirror & Phasing Actuators

The last sensitivity study performed was on the primary mirror parameters and the phasing actuators. Two parameters were examined: the primary membrane mirror areal density and the electron gun area coverage. Although cabling for the e-guns was identified as a significant amount of the primary mirror weight, an increase in the e-gun coverage would reduce the number of guns and thus reduce the amount and weight cabling needed. Also, it was assumed that the e-guns were mounted to the secondary mirror assembly, meaning that the e-gun weight did not affect the aperture areal density. The number of guns does, however, affect the total estimated satellite weight. For this sensitivity study, the torus support structure was used.

Figure 4.3-1 demonstrates the effect the membrane areal density has on the total areal density. As expected, the total aperture areal density is directly proportional to the membrane areal density. The non-zero y-intercept demonstrates the overhead weight associated with support hardware for the membrane system. Another reason for the linear relationship is that the torus support structure analysis lacks any feedback on sizing this system. No attempt was made to analyze the torus's structural properties for changing loads or slew requirements.

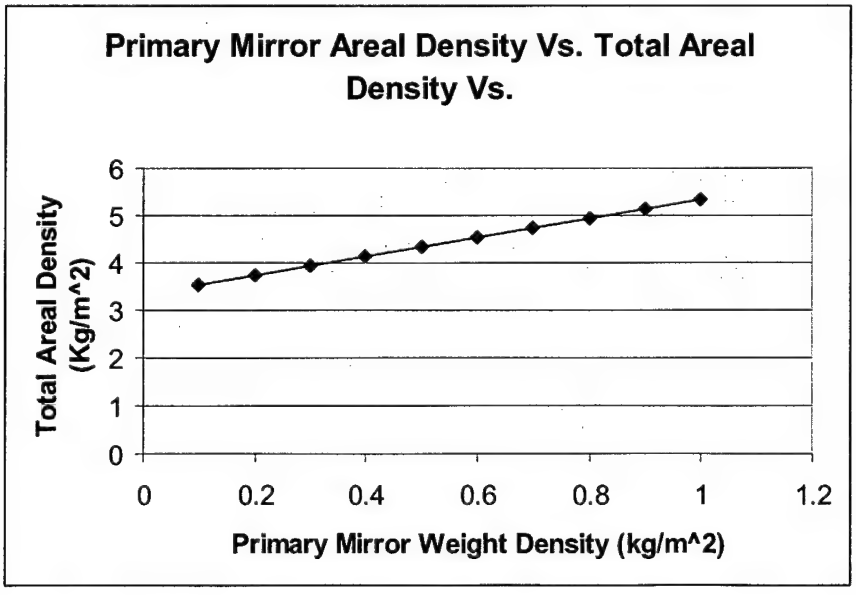

Figure 4.3-1. Mirror areal density versus total areal density

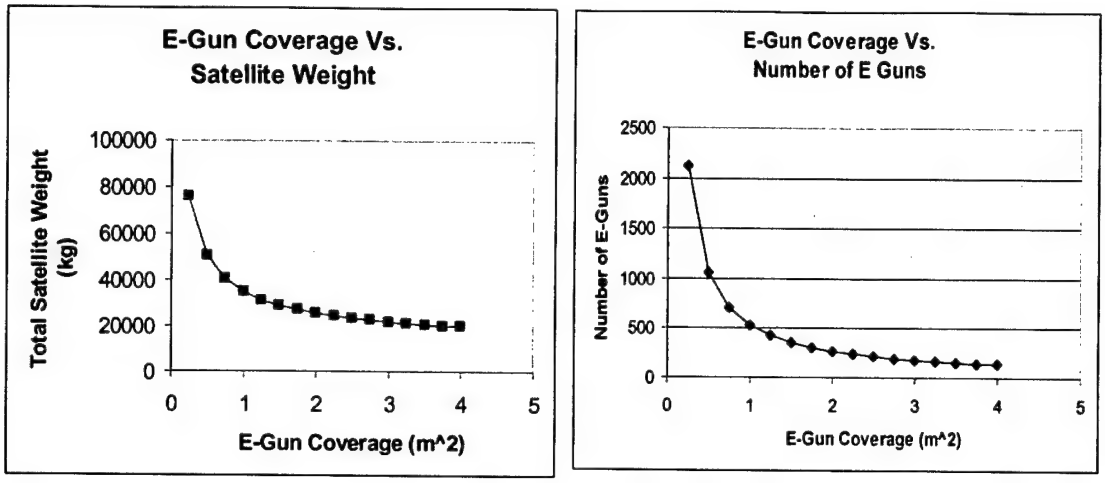

Figure 4.3-2. E-Gun coverage versus total satellite weight and number of E-Guns

Figure 4.3-2 shows the effect of the e-gun coverage on the system weight and number of guns needed. The coverage strongly affects both the system weight and the number of guns needed. Notice that as the coverage doubles from 0.25 meters squared to 0.5 meters squared that the number of e-guns decreases by a factor of 2 and the total satellite weight drops by 30%. Of course, the real returns on increased e-gun coverage quickly begin to shallow around coverage numbers of 2 meters squared, but this is expected.

4.4 Sensitivity of System Parameters to Aperture Size

The final question is how does the areal density and total satellite weight change with aperture size. First, the parameters varied during the sensitivity studies were set to assumed values. Next, the aperture diameter was varied and the primary mirror areal density and total system weight recorded. Table 4.4-1 shows the system parameters constants used for this study.

Table 4.4-1. Sensitivity parameters in aperture study

Parameter Name	Nominal Value	Units	Reason for Value
Type of Primary Mirror Support Structure	Torus	(none)	Best Support
E-Gun Coverage	4	M^2	Not an unreasonable value
Membrane Areal Density	0.1	Kg/m^2	Traceable to known H/W
Torus Weight Margin	9	(none)	System specified to weight 10 times estimated weight is very conservative

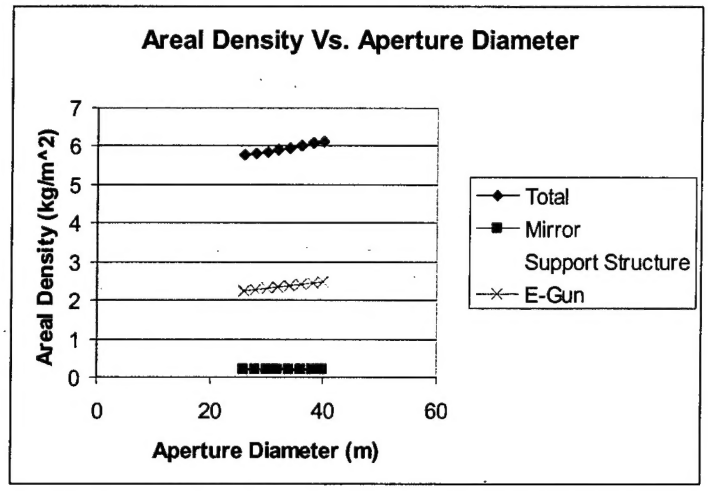

Figure 4.4-1. Aperture diameter versus primary mirror areal density. Primary mirror areal density includes the weight of the electron gun systems mounted on the secondary mirror assembly.

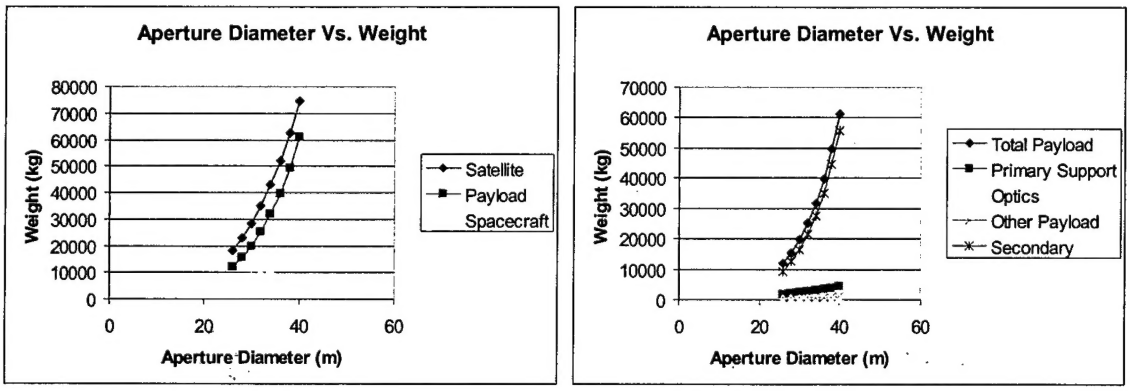

(a) (b)

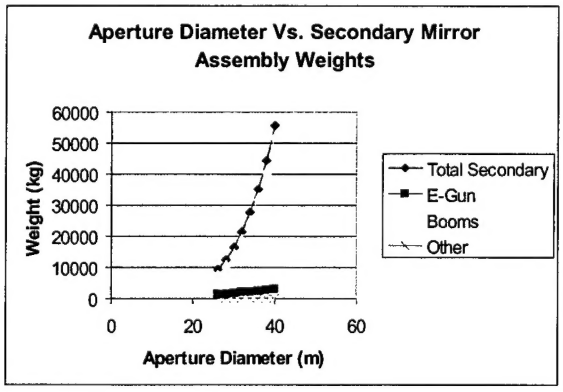

(c)

Figure 4.4-2. Aperture diameter versus weight

Figures 4.4-1 and 4.4-2 shows the results of the areal density and system weight studies. The primary mirror aperture areal density results shown that areal density is weakly related to aperture diameter. The flat nature of the graph is somewhat surprising considering the two major primary mirror weight factors, membrane weight and number of electron guns, are both proportional to the aperture area which is related to the square of the aperture diameter. However, figure 4.4-1 does demonstrate a linear relationship between aperture size and areal density as expected.

One other noticeable characteristic of Figure 4.4-1 is what it states about the technology development needs and impacts. From Figure 4.2-1 the primary mirror support structure constitutes 3 kilograms per meter squared of the total areal density for a margin factor of 9. If the estimated weights before the margin factor are correct, then the overall areal density drops to nearly 3 kilograms per meter squared. Similarly, if figure control is not needed because a real-time holography system can remove the figure errors, then the areal density drops 2 to 2.5 kilograms per meter squared. Optimistically, the areal density could be well below one if real-time holography and torus support structures mature.

In comparison to the primary mirror areal density study, the system weight study shows a stronger relationship between aperture size and aperture diameter. Figure 4.4-2 shows the results of that study. Notice that the secondary mirror booms drive most of the satellite weight. A system-by-system weight breakdown is shown from Figure 4.4-2a down to Figure 4.4-2c.

Further examination of the secondary assembly boom weight calculations revealed that the lateral frequency requirement was forcing a high boom thickness and thus a high boom mass. Eliminating the electron guns from the secondary assembly reduced the mass by 50%. Further sensitivity analysis discovered, similar to the primary mirror booms, that the radius to thickness ratio could be increased to reduce the boom mass. More detailed design work on the booms needs to be performed to flush out this issue.

5. Conclusions

A systems-engineering model has been built to examine Gossamer, imaging systems. A sensitivity analysis was also performed that looked at how parameter design changes effected the overall weight and performance. Several surprises came out of that study:

1). **Given that the performance is similar, torus support structures are superior to thin-walled tube support structures. However, more structurally efficient boom systems such as solid wall trusses, isogrids, and tubular trusses need to be examined.** Thin walled tube support structures use too much material and therefore weigh more than torus type of primary mirror support structures. However, thin-walled tubular booms are not very structurally efficient. An expanded database to include these structures needs to be developed.

2). **Most of the aperture areal density is not tied to the mirror system.** Most of the weight of a membrane system is in the support structure and figure control hardware. Technology development that reduces or more accurately determines these weights is needed.

3). **Using a primary mirror torus support structure, a significant amount of the payload weight is composed of the secondary mirror support structure.** More detailed design work on the secondary mirror support booms is needed to determine their actual weight to meet performance requirements.

6. References

[1]. Bell, Kevin, "Assessment of a Large Aperture Telescope Trade Space and Active Opto-Mechanical Control Architecture," IEEE Aerospace Conference, 1997

[2]. Bell, Kevin, "Balancing High Performance and Low Cost for Satellite System Design Using an Integrated Concurrent Engineering Model," EUROOPTO 95.

[3]. "Gossamer Spacecraft: Membrane and Inflatable Structures Technology for Space Applications", Progress in Astronautics and Aeronautics, Volume 191, AIAA, Reston, VA, 2001.

[4]. Larson, W. J., & Wertz, J. R., "Space Mission Analysis and Design", Kluwer Academic Publishers, Boston, MA, 1993.

[5]. Aleksandrov, A. D., et al., "Mathematics: Its Content, Methods and Meaning", Volume 1, Dorset Press, New York, NY, 1990.

[6]. "Astronautic Structures Manual", NASA TM X 73306, Structures and Propulsion Laboratory, NASA Marshall Space Flight Center, August 1975.

[7]. Main, J. A., Nelson, G. C., & Martin, J. W., "Electron Gun Control of Piezoelectric Materials", SPIE Symposium on Smart Structures and Materials, SPIE, 1998.

DISTRIBUTION LIST

DTIC/OCP 8725 John J. Kingman Rd, Suite 0944 Ft Belvoir, VA 22060-6218	1 cy
AFRL/VSIL Kirtland AFB, NM 87117-5776	2 cys
AFRL/VSIH Kirtland AFB, NM 87117-5776	1 cy
Official Record Copy AFRL/VSSV/Lawrence Robertson	3 cys